Numerical simulations of subionospheric VLF propagation under influence of moderate Solar X-ray flare events

Aleksandra Kolarski

Institute of Physics, University of Belgrade, Pregrevica 118, 11000 Belgrade, Serbia
E-mail: aleksandra.kolarski@ipb.ac.rs

Abstract

Soft X-ray radiation (0.1-0.8 nm) from Solar flare events, as one of the most important ionizing agents within D-region altitude range (50-90 km) of the sunlit lower Ionosphere, causes perturbations in subionospheric propagation of manmade Very Low Frequency (VLF) radio signals. Based upon VLF signal perturbations, by the use of the Long Wave Propagation Capability (LWPC) software relaying on Wait's theory, remote sensing of the lower Ionosphere from ground based stations is a well established research method. Subionospheric VLF propagation under influence of moderate Solar X-ray flare events (C and M class) during descending phase of the 23rd Solar cycle were analyzed on two VLF traces, simultaneously recorded by narrowband recording station in Belgrade (44.85N, 20.38W), Serbia. Influences of moderate Solar flares were inspected on one relatively short GQD/22.1 kHz and one relatively longer NAA/24 kHz VLF signal paths, with focus on numerical simulations of their propagation characteristics.

Introduction

The majority of ionospheric electron content lies within atmospheric thermosphere altitude range. Ionospheric layers significantly differ according to characteristics, constituents, variations, ionization processes involved etc. Ionospheric D-region is the innermost ionospheric layer, with the bulk of its electron content contained within altitude height range 50-90 km, within atmospheric mesosphere region. Since situated closest to the Earth's surface, D-region is both influenced by the incident energy flux originated from Sun and outer space, and by the coupling with terrestrial processes. X-ray spectral range of Solar radiation penetrates deep into the Earth's atmosphere and is one of the most important factors regarding the space weather. X-rays in wavelengths range 0.1-1 nm can reach heights with ionospheric D-region constituents, and thus are of the great importance as ionizing agent within this region during daytime. In quiet ionospheric conditions, production of electrons within D-region is mainly under

photoionization processes, UV Lyman-α spectral line 121.6 nm, EUV spectral lines ranging from 102.7 nm to 118.8 nm and galactic cosmic rays (e.g. Thomson et al. 2021 and references therein). Electromagnetic radiation during Solar flare events emitted in soft X-ray range (0.1–0.8 nm) causes photoionization of all neutral constituents within D-region and considerably exceeds ionization produced by regular factors (Lyman- α spectral line and cosmic rays), becoming a major ionization source in this region (Whitten and Poppoff 1965, Hargreaves 1992). Due to additional ionization, electron density within D-region increases, affecting the characteristics of the Earth-Ionosphere waveguide (Mitra et al. 1974).

Analysis and results

One of methods for investigating lower Ionosphere is utilization of manmade radio-signals in frequency range 3-30 kHz, belonging to the Very Low Frequency (VLF) range. These signals are globally emitted, usually by the military transmitters and for the military purposes, with stable signal and mainly in continual mode. This makes them very suitable for use in scientific purposes, as the remote sensing technique for monitoring of the lower Ionosphere. VLF signals transmit within Earth-Ionosphere waveguide, with stable amplitude and phase delay in quiet solar conditions (Budden 1988, Thomson 1993, McRae and Thomson 2000). Changes in electron density height profile within D-region, due to incident Solar X-ray radiation during solar flare events, influence propagation conditions within Earth-Ionosphere waveguide causing perturbations of VLF signals' amplitude and/or phase delay. Not only driven by Solar X-ray flares, VLF signal perturbations can also be driven by many other phenomena originating from extraterrestrial (e.g. γ-ray bursts, coronal mass ejections, solar eclipse etc.) to terrestrial (e.g. coupling with lightning activity, volcano eruptions, earthquakes, hurricanes etc.) environment. Many research groups dealt with topic of monitoring lower ionospheric features based upon the use of artificial VLF radio signals and their propagation characteristics (e.g. Silber and Price 2017 and references therein).

Utilization of Long Wave Propagation Capability (LWPC) numeric program package (Ferguson et al. 1998), based upon Wait's theory (Wait and Spies 1964, Wait 1970), and integrated with measured VLF data, has confirmed as successful technique for exploration of lower Ionosphere by many researchers (e.g. Thomson et al. 2011, 2005, McRae and Thomson 2000, 2004, Pal and Chakrabarti 2010, Basak and Chakrabarti 2013, Žigman et al. 2007, Grubor et al. 2008, Nina et al. 2011, 2012, 2018, Nina and Čadež 2014, Kolarski and Grubor 2014, 2015, Kolarski et al. 2011, 2022, Kumar and Kumar 2018, Šulić et al. 2016, Šulić and Srećković 2014, Srećković et al. 2021, Chowdhury et al. 2021 etc). Monitoring of ionospheric D-region during Solar flare events of moderate intensity from descending phase of the 23rd Solar cycle, as observed on two VLF signal traces simultaneously registered in Belgrade was conducted in this paper, with focus on numerical modeling procedure applied.

Influences of moderate intensity Solar flare events of C and M class, during descending phase of the 23rd Solar cycle, were analyzed on subionospheric VLF propagation on GQD and NAA VLF signal traces, as recorded in Belgrade (44.85N, 20.38E), at the Institute of Physics, by narrowband Absolute Phase and Amplitude Logger (AbsPAL) receiving station. GQD/22.1 kHz signal arrives from UK (Skelton (54.72N, 2.88W)) along relatively short and mostly an overland propagation path (GCP_{GQD}=1982 km), from WNW-ESE direction towards Belgrade, while NAA/24 kHz VLF signal arrives from USA (Maine (44.63N, 67.28W)) along relatively longer and mostly an oversea propagation path (GCP_{NAA}=6540 km), from W-E direction towards Belgrade. Solar X-ray irradiance data are taken from the website of National Oceanic and Atmospheric Administration (NOAA), from Geostationary Operational Environmental Satellite (GOES) Network database, from link: https://www.ngdc.noaa.gov/stp/satellite/goes/index.html.

Numerical simulations of propagation characteristics along their GCPs, under influence of analyzed C&M class Solar flare events, were conducted using LWPC software package, based on real measured amplitude and phase delay VLF data in Belgrade. During simulation process, the goal was to obtain simulated data, to fit as close as possible, to real measured data. Numerical simulations of subionospheric VLF propagation were carried out in ionospheric conditions before the influence of observed Solar flare events, denoted as *preflare state*, during the time evolution of each observed flare's influence on monitored VLF signal propagation, with *flare state* denoting the moment that corresponds to maximal X-ray irradiance i.e. I_{Xmax} and in ionospheric conditions recovered after the influence of observed Solar flare events, denoted as *postflare state*.

According to the Wait′s theory, electron density *Ne* (m^{-3}) height profiles within the Earth-Ionosphere waveguide at the altitude z (km), are determined by pairs of parameters, denoted as reflecting edge *sharpness* β (km^{-1}) of the lower boundary of the Ionosphere and *reflecting height H′* (km). Based upon exponential model of the Ionosphere, incorporated into LWPC software, unperturbed daytime ionospheric conditions are defined by parameter pair (β, *H′*) being held constant (0.3, 74) along entire propagation path. Perturbed ionospheric conditions are reproduced by modeling parameter pairs (β, *H′*) along propagation path, as manually entered values into REXP subroutine, with goal to get program's output amplitude and phase delay values as closest as possible to real measured VLF data at the receiver site. For purposes of obtaining *Ne* (m^{-3}), relation designed for daytime Ionospheric conditions based on Wait′s theory, was used:

$$Ne(z, H', \beta) = 1.43 \cdot 10^{13} \cdot e^{-0.15H'} \cdot e^{(\beta-0.15)(z-H')}. \quad (1)$$

Some of the numerically modeled parameters for subionospheric propagation of NAA and GQD signal traces for analyzed Solar flare events are given in Table 1, while electron density *Ne* (m^{-3}) height profiles in *flare states* are given in Fig. 1.

Table 1. NAA and GQD signal traces modeled parameters for analyzed Solar flares

Analyzed Solar flare events	Date (y/m/d)	06/04/07	06/07/06	05/09/07	06/12/06
	TimeUT (hh:mm)	08:03	08:36	12:44	12:58
	Class	C9.7	M2.5	C9.6	C4.8
	I_{Xmax} (Wm^{-2})	$9.74\cdot10^{-6}$	$2.51\cdot10^{-5}$	$9.62\cdot10^{-6}$	$4.82\cdot10^{-6}$
preflare conditions	NAA GQD	regular	regular	perturbed	perturbed
Quiet day (y/m/d)	NAA GQD	06/04/08	06/07/05	06/09/10 05/09/08	06/11/24 06/12/08
$\beta_{preflare}$ (km^{-1})	NAA GQD	0.30 0.33	0.361 0.28	0.432 0.335	0.253 0.425
β_{flare} (km^{-1})	NAA GQD	0.50 0.45	0.545 0.455	0.57 0.385	0.315 0.53
$\beta_{postflare}$ (km^{-1})	NAA GQD	0.375 0.325	0.392 0.32	0.425 0.325	0.22 0.355
$H'_{preflare}$ (km)	NAA GQD	74 72.5	74.1 75	73.3 71	71.3 72
H'_{flare} (km)	NAA GQD	67 69	69 65.5	70 66.5	66.6 70
$H'_{postflare}$ (km)	NAA GQD	72 72.5	73 72	73.4 72	74.2 72.8
$Ne_{preflare}$(65km) (m^{-3})	NAA GQD	$5.60\cdot10^{7}$ $7.02\cdot10^{7}$	$3.12\cdot10^{7}$ $5.07\cdot10^{7}$	$2.31\cdot10^{7}$ $1.12\cdot10^{8}$	$1.69\cdot10^{8}$ $4.26\cdot10^{7}$
$Ne_{preflare}$ (75 km) (m^{-3})	NAA GQD	$2.51\cdot10^{8}$ $4.24\cdot10^{8}$	$2.57\cdot10^{8}$ $1.86\cdot10^{8}$	$3.88\cdot10^{8}$ $7.10\cdot10^{8}$	$4.74\cdot10^{8}$ $6.66\cdot10^{8}$
$Ne_{preflare}$ (80 km) (m^{-3})	NAA GQD	$5.31\cdot10^{8}$ $1.04\cdot10^{9}$	$7.39\cdot10^{8}$ $3.56\cdot10^{8}$	$1.59\cdot10^{9}$ $1.79\cdot10^{9}$	$7.94\cdot10^{8}$ $2.63\cdot10^{9}$
Ne_{flare}(65 km) (m^{-3})	NAA GQD	$3.07\cdot10^{8}$ $1.38\cdot10^{8}$	$9.42\cdot10^{7}$ $6.64\cdot10^{8}$	$4.82\cdot10^{7}$ $4.68\cdot10^{8}$	$5.04\cdot10^{8}$ $5.89\cdot10^{7}$
Ne_{flare}(75 km) (m^{-3})	NAA GQD	$1.02\cdot10^{10}$ $2.77\cdot10^{9}$	$4.89\cdot10^{9}$ $1.40\cdot10^{10}$	$3.22\cdot10^{9}$ $4.91\cdot10^{9}$	$2.62\cdot10^{9}$ $2.63\cdot10^{9}$
Ne_{flare}(80 km) (m^{-3})	NAA GQD	$5.84\cdot10^{10}$ $1.24\cdot10^{10}$	$3.53\cdot10^{10}$ $6.44\cdot10^{10}$	$2.63\cdot10^{10}$ $1.59\cdot10^{10}$	$5.98\cdot10^{9}$ $1.76\cdot10^{10}$
$Ne_{postflare}$ (65 km) (m^{-3})	NAA GQD	$6.04\cdot10^{7}$ $7.28\cdot10^{7}$	$3.62\cdot10^{7}$ $8.87\cdot10^{7}$	$2.35\cdot10^{7}$ $8.57\cdot10^{7}$	$1.10\cdot10^{8}$ $5.22\cdot10^{7}$
$Ne_{postflare}$ (75 km) (m^{-3})	NAA GQD	$5.73\cdot10^{8}$ $4.19\cdot10^{8}$	$4.07\cdot10^{8}$ $4.86\cdot10^{8}$	$3.67\cdot10^{8}$ $4.93\cdot10^{8}$	$2.22\cdot10^{8}$ $4.06\cdot10^{8}$

$Ne_{postflare}$ (80 km) (m^{-3})	NAA GQD	$1.76 \cdot 10^9$ $1.01 \cdot 10^9$	$1.37 \cdot 10^9$ $1.14 \cdot 10^9$	$1.45 \cdot 10^9$ $1.18 \cdot 10^9$	$3.15 \cdot 10^8$ $1.13 \cdot 10^9$

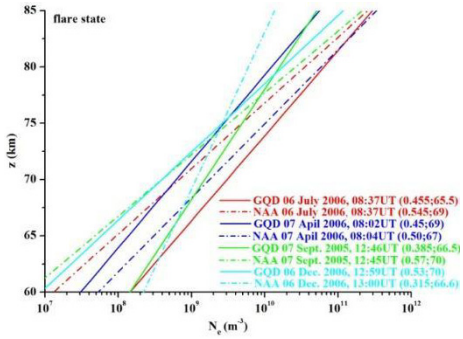

Fig. 1. Electron density height profiles for analyzed Solar flares in *flare states* for GQD and NAA signals, with corresponding modeled parameters (β, *H*′)

Conclusions

Conducted numerical simulations of subionospheric VLF propagation of GQD and NAA signals, based on Wait′s parameters and LWPC calculations, under the influence of chosen moderate C&M class Solar X-ray flare events from descending phase of the 23rd Solar cycle presented in this paper, are in good agreement with real measured VLF data at the place of the Belgrade AbsPAL receiver. It can be assumed, that numerically simulated average ionospheric conditions, held along GQD and NAA signal paths, realistically reproduce real ionospheric conditions, both for *preflare states* as for perturbed *flare states*, as well as for recovered *postflare states* in both waveguides and that applied modeling technique based on Wait′s theory and LWPC software utilization gives good modeling results for the purposes of qualitative analysis. Obtained results are in line with other studies performed by same technique for mid-latitude Ionosphere (e.g. Grubor et al. 2008, Žigman et al. 2007, McRae and Thomson 2004, Nina et al. 2012, Palit et al. 2013, Kolarski et al. 2015, 2022 etc.). Pattern, morphology and complexity of recorded signals' perturbations, forced by observed X-ray Solar flare events, differ for monitored GQD and NAA signal traces, since propagation differences within their waveguides, but also due to diurnal and seasonal ionospheric factors and X-ray Solar flare events' characteristics (Grubor et al. 2008). In general, GQD signal responds to soft Solar X-ray radiation of moderate intensity in more complex manner, with multiple amplitude and phase delay signal's extremes, compared to quite simple NAA response, with one maximum that corresponds to maximal X-ray irradiance. However, time delay Δt (Žigman et al. 2007) in signal reaching the maximum of X-ray Solar flare irradiance, for all analyzed cases, is up to 2 minutes.

Acknowledgments

Author thanks D. Grubor and D. Šulić. Thanks are due to The Ministry of Education, Science and Technological Development of the Republic of Serbia.

References

Basak, T., Chakrabarti, S. K., 2013, Astrophys. Space Sci., 348, 2, pp. 315–326.
Budden, K. G., 1988, The propagation of radio waves, Cambridge Univ. Press UK.
Chowdhury, S., Kundu S., Basak, T., Ghosh S., Hayakawa, M., Chakraborty S., Chakrabarti, S. K., Sasmal, S., 2021, ASR, 67, 1599–1611.
Ferguson, A. J., 1998, Computer program for assessment of long-wavelength radio communications, Version 2.0., Technical document 3030, Space and Naval Warfare Systems Center, San Diego CA 92152-5001, USA.
Grubor, D. P., Šulić, D. M., Žigman, V., 2008, Ann. Geophys., 26, 1731–1740.
Hargreaves, J. K., 1992, The solar-terrestrial environment, Cambridge Univ. Press.
Kolarski, A., Grubor, D., 2014, ASR, 53, 11, 1595 – 1602.
Kolarski, A., Grubor, D., 2015, J. Astrophys. Astr., 36, 4, 565–579.
Kolarski, A., Grubor, D., Šulić, D., 2011, Baltic Astron., 20, 591–595.
Kolarski, A., Srećković, V. A., Mijić, Z. R., 2022, Appl. Sci., 12, 582.
Kumar, A., Kumar, S., 2018, EPS, 70-29.
McRae, W. M., Thomson, N. R., 2000, JASTP, 62, 609–618.
McRae, W. M., Thomson, N. R., 2004, JASTP, 66, 77–87.
Mitra, A. P., 1974, Ionospheric effects of solar flares. Astrophysics and Space Science Library, vol. 46, D. Reidel publishing Company, Boston, USA.
Nina, A., Čadež, V. M., 2014, ASR, 54, 7, 1276-1284.
Nina, A., Čadež, V. M., Bajčetić, J., Mitrović, S. T., Popović, L. C., 2018, Sol. Phys., 293, 64
Nina, A., Čadež, V., Srećković, V. A., Šulić, D., 2011, Baltic Astron., 20, 609–612.
Nina, A., Čadež, V., Šulić, D., Srećković, V., Žigman, V., 2012B, Methods Phys. Res. B, 279, 106–109.
Pal, S., Chakrabarti, S. K., 2010, AIP Conf. Proc. 1286, 1, 42–60.
Silber, I., Price, C., 2017, Surv. Geophys., 38(2), 407–441.
Srećković, V. A., Šulić, D.M., Ignjatović, L., Vujčić, V., 2021, Appl. Sci. 11, 7194.
Thomson, N. R., 1993, JASTP, 55 (2), 173–184.
Thomson, N. R., Clilverd, M. A., Brundell, J. B., Rodger, C. J., 2021, J. Geophys. Res. Space Phys., 126, 10.1029/2020JA029043.
Thomson, N. R., Rodger, C. J., Cliverd, M. A., 2005, JGR, 110, A06306.
Thomson, N. R., Rodger, C. J., Clilverd, M. A., 2011, JGR, 116, 11305–11310.
Wait, R. J., 1970, Electromagnetic Waves in Stratified Media, Pergamon Press, Oxford, UK.
Wait, R. J., Spies, K. P., 1964, Characteristics of the Earth-Ionosphere waveguide for VLF radio waves, NBS Technical Note 300, USA.

Whitten, R. C., Poppoff, I. G., 1965, Physics of the Lower Ionosphere, Englewood Cliffs, N.J. Prentice-Hall, USA.
Šulić, D., Srećković, V. A, 2014, SAJ, 188, 45-54.
Šulić, D. M., Srećković, V. A., Mihajlov, A. A., 2016, ASR, 57, 1029–1043.
Žigman, V., Grubor, D., Šulić, D., 2007, JASTP, 69, 775–792.